Ionospheric density variations recorded before the 2010 Mw 8.8 earthquake in Chile

D Píša, Michel Parrot, O Santolík

Ionospheric density variations recorded before the 2010 M_w 8.8 earthquake in Chile

D. Píša,[1,2,3] M. Parrot,[1] and O. Santolík[2,3]

Received 3 March 2011; revised 20 July 2011; accepted 22 July 2011; published 18 August 2011.

[1] We present a study of plasma density variations observed by the DEMETER spacecraft in the vicinity of a very powerful earthquake in Chile. This earthquake of moment magnitude 8.8 occurred on 27 February 2010 with an epicenter located at 35.85°S, 72.72°W. Data recorded 10–20 days before the main shock along orbits close to the future epicenter show increasing plasma densities. In a second step, a statistical analysis with DEMETER data has been performed using the first 3 months of the years 2007–2010 to monitor density variations in the vicinity of the epicenter at the same local time and seasonal conditions. This study shows that a large increase of the plasma density is very uncommon at this location and at this time and that the increases observed during the days before the main shock could be considered as possible short-term precursors of this powerful earthquake.

Citation: Píša, D., M. Parrot, and O. Santolík (2011), Ionospheric density variations recorded before the 2010 M_w 8.8 earthquake in Chile, *J. Geophys. Res.*, *116*, A08309, doi:10.1029/2011JA016611.

1. Introduction

[2] Observations of phenomena related with the seismic activity represent a very relevant topic because once again a series of strong and damaging earthquakes recently occurred around the world. Many efforts are done to find effects which can be considered as possible short-term precursors. Authors have recently discussed the electromagnetic wave perturbations possibly connected with the seismic activity using ground-based data [*Tate and Daily*, 1989; *Asada et al.*, 2001; *Hattori*, 2004] and satellite data [*Parrot and Mogilevsky*, 1989; *Larkina et al.*, 1989; *Parrot*, 1994]. In general, it is very difficult to show which perturbations are connected to earthquakes because they are weak and often superposed on more powerful signals for example related to lightning strokes. Therefore some authors tried to eliminate these effects by statistical studies of electromagnetic field variations which can remove the influence of ambient noises [*Parrot*, 1999; *Němec et al.*, 2008, 2009].

[3] There are many theories involving a lithosphere-atmosphere-ionosphere coupling to explain these ionospheric perturbations. They can be found in work by *Pulinets and Boyarchuk* [2004, and references therein]: Direct wave production in a wide band spectrum by compression of rocks close to earthquake epicenter (it could be likely related to piezoelectric and triboelectric effects); Rising fluids under the ground which can lead to emanation of warm gases; Heating and propagation of acoustic-gravity waves; Activation of positive holes that can reach the ground surface (see the review paper by *Freund* [2009]); Emissions of radioactive gas or metallic ions such as radon lead to increase the potential at the Earth's surface [*Harrison et al.*, 2010]. This thin layer of particles created before earthquakes due to ion radiation from the Earth has a main role in transferring electric field to the above atmosphere and then to the ionosphere. The penetration of this electric field in the ionosphere could induce plasma density anomalies, which are observed in the earthquake area [see, e.g., *Liu et al.*, 2006; *Kon et al.*, 2011]. Acoustic-gravity wave (AGW) could also trigger pre-earthquake ionospheric perturbations [see, e.g., *Liu et al.*, 2008]. Just after the earthquake it is well known that it is the AGW raised by the shock which perturbs the ionosphere [*Blanc*, 1985].

[4] The purpose of this paper is to present a statistical analysis of the ionospheric density observed by the DEMETER satellite around the time of a large earthquake in Chile. The area along Chile's coast is one of the most active seismic zones around the world. It is due to the very fast relative motion (up to 130 mm/y) of the Nazca and the South American tectonic plates [*Norabuena et al.*, 1999]. The M_w 8.8 Chile earthquake which occurred on 27 February 2010 is the second largest event since the launch of DEMETER. Its epicenter was located at 35.85°S, 72.72°W and the depth was 35 km. The fact that this powerful earthquake occurred during and after a long period of very low solar activity provides a unique opportunity to check its effects on the ionosphere and to perform a statistical analysis. The DEMETER payload is briefly described in section 2. In section 3, three individual events which occurred 17, 11, and 9 days before the main shock are shown. The results of the

[1]LPC2E, CNRS, Orléans, France.
[2]IAP, ASCR, Prague, Czech Republic.
[3]Faculty of Mathematics and Physics, Charles University, Prague, Czech Republic.

0148-0227/11/2011JA016611

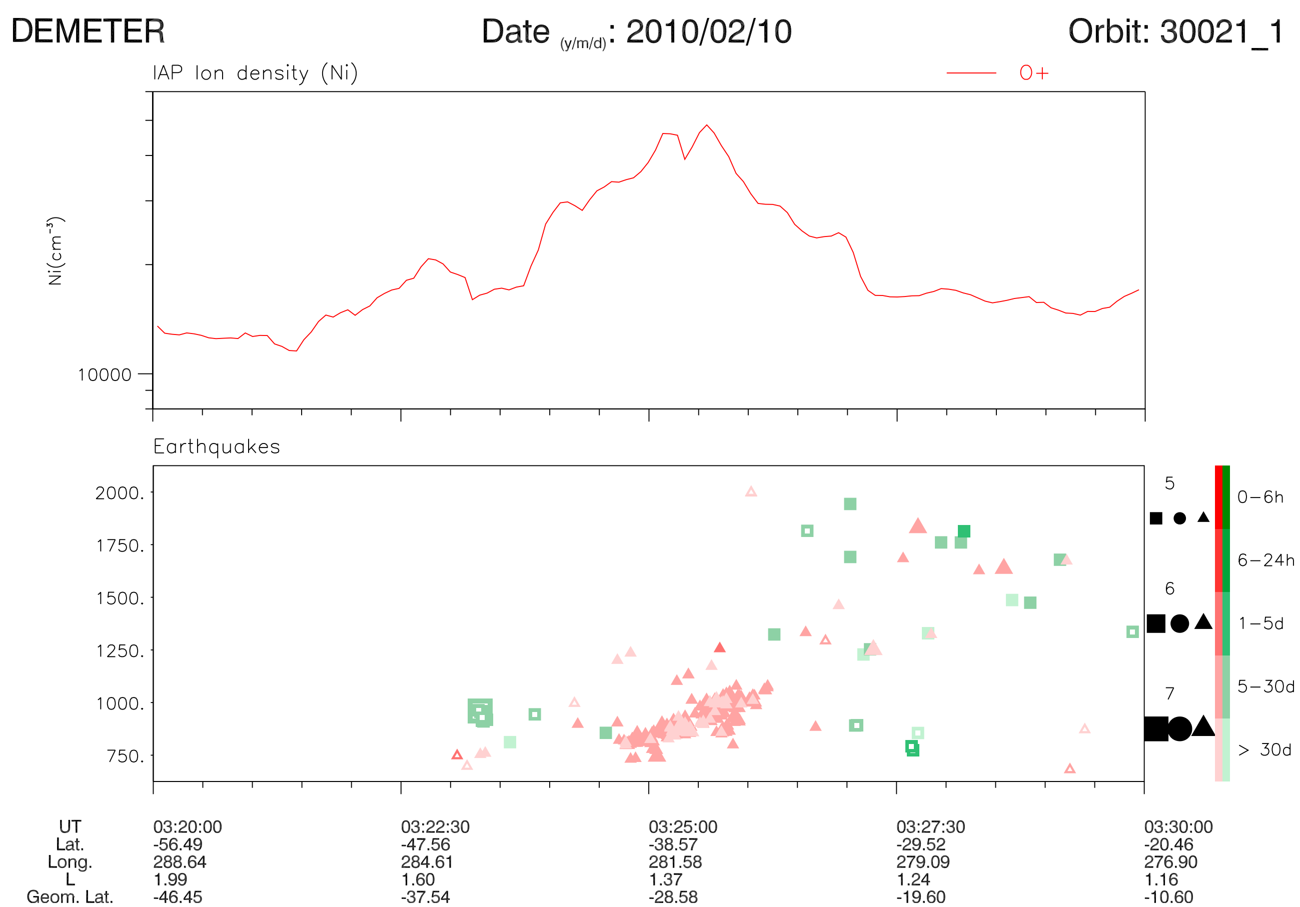

Figure 1. Data recorded on 10 February 2010 between 03:20:00 and 03:30:00 UT. (top) The density of the ion O^+. The densities of the ions H^+ and He^+ are much lower than the density of the ion O^+, and they do not appear within the given density range. (bottom) The distance and magnitude of coming earthquakes as a function of the time. The red triangles are related to the future main shock and to the future aftershocks (see the text for more explanations about the symbols). The closest approach to the main shock is at 03:25:30 UT. The parameters below the plots indicate that the observation takes place during nighttime along the rupture zone of the earthquakes in Chile.

statistical analysis are presented in section 4. Discussion and conclusions are provided in section 5.

2. The Experiment

[5] DEMETER is a low-altitude satellite (710 km) launched in June 2004 into a polar and circular orbit. It measures electromagnetic waves and plasma parameters all around the globe except in the auroral zones [*Parrot*, 2006]. The altitude of the satellite was decreased to 660 km in December 2005. Due to technical reasons data are only recorded at invariant latitudes less than 65°. The orbit of DEMETER is nearly Sun-synchronous and the northward half-orbits correspond to nighttime (22:30 LT) whereas the southward half-orbits correspond to daytime (10:30 LT). Variations of the ion density are measured by the instrument IAP (Instrument Analyseur de Plasma). IAP is fully described by *Berthelier et al.* [2006]. Observations of ionospheric perturbations and their interpretation as possible short-term precursors of earthquakes represent the main scientific objective of DEMETER.

3. DEMETER Observations

[6] Due to its orbit, DEMETER returns every day above the same region but more or less close to a given point (epicenter). The ion density shown in Figure 1 has been recorded by the satellite along an orbit close to the epicenter on 10 February 2010, i.e., 17 days before the earthquake. Figure 1 (top) shows the O^+ ion density obtained from IAP. Figure 1 (bottom) shows symbols of coming earthquakes with their distances from the satellite, magnitudes and times to the shock. The symbols are filled green squares for past earthquakes and aftershocks, filled red triangles for earthquakes and aftershocks which will occur soon close to the half-orbit. The color scales on the right (green and red) give the time interval between the earthquakes and the DEMETER orbit with a color gradation from >30 days up to a [0–6 h] interval. The empty symbols have similar sig-

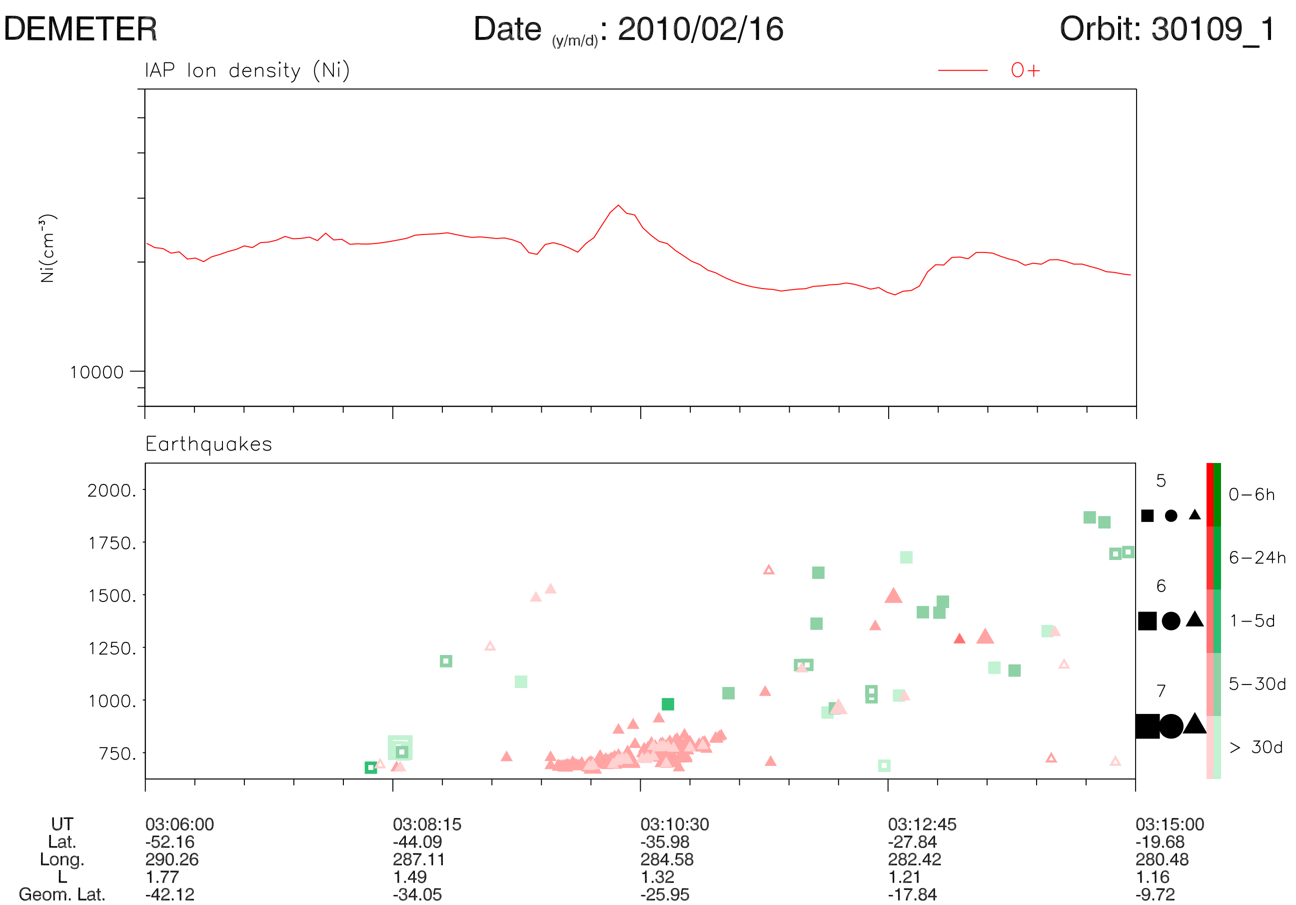

Figure 2. Data recorded on 16 February 2010 between 03:06:00 and 03:15:00 UT. The format is the same as in Figure 1. The closest approach to the main shock is at 03:10:17 UT.

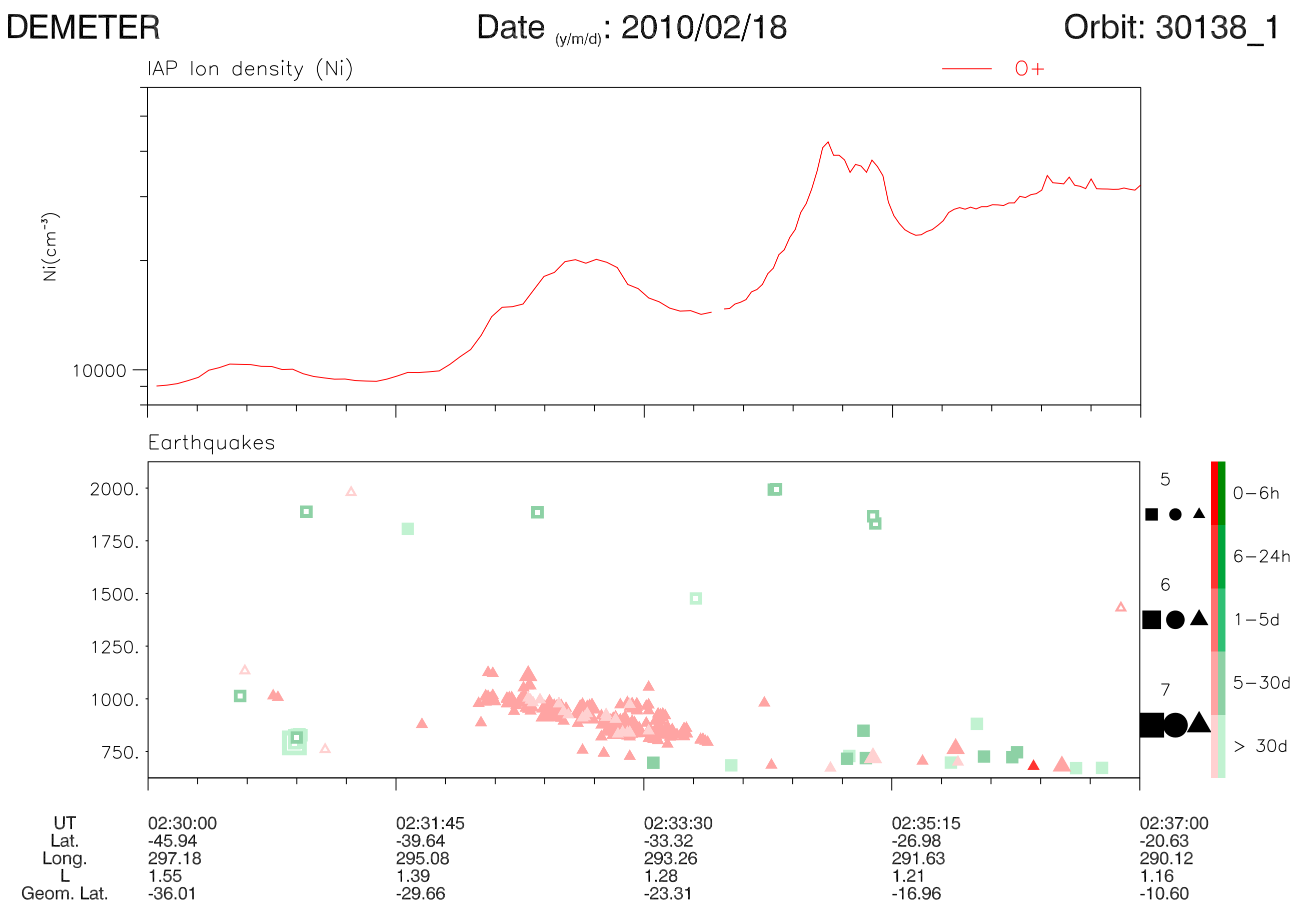

Figure 3. Data recorded on 18 February 2010 between 02:30:00 and 02:37:00 UT. The format is the same as in Figure 1. The closest approach to the main shock is at 02:33:08 UT.

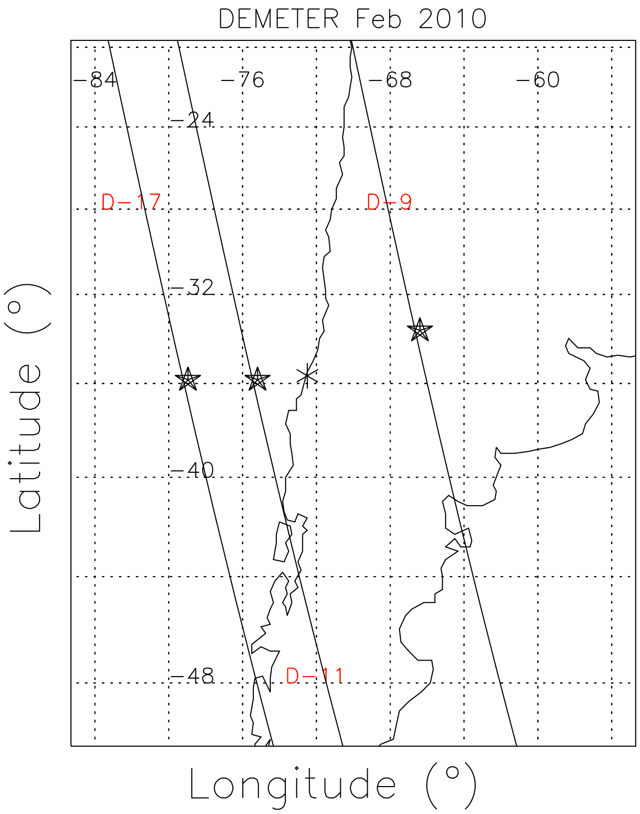

Figure 4. Traces of the orbits whose data are shown in Figures 1–3. The epicenter is indicated by an asterisk. The stars on each trace indicate the location where the maximum of the signal is observed.

nifications except that they are related to the conjugate points of the epicenters (the distance D is then the distance between the conjugate points of the epicenters and the satellite). The symbol sizes correspond to earthquakes of magnitude [5–6], [6–7], and [>7]. In Figure 1 (bottom), the numerous red filled triangles are related to the future main shock and to the future aftershocks, and their elongated positions indicate that the DEMETER orbit is almost parallel to the rupture fault. The electron density and the O^+ ion density have the same variation (not shown). These densities present a clear local maximum around 03:25 UT, vertically above the future epicenter. Figure 2 displays the data recorded on 16 February 2010, i.e., 11 days before the earthquake. The format is the same as Figure 1, and it can be observed that the O^+ ion density presents a maximum above the epicenter. Figure 3 shows the data recorded on 18 February 2010, i.e., 9 days before the earthquake. The format is the same as in Figure 1. During the whole time interval, the density globally increases and presents two local maxima. The first maximum is at 02:33:05 UT, and Figure 1 (bottom) indicates that it corresponds to the middle of the rupture zone. The second density maximum occurs between 02:34:47 and 02:35:06 UT. Using the IGRF magnetic field model it occurs that this second maximum is located at the magnetically conjugate point of the epicenter at the altitude of the satellite (660 km). This indicates that the earthquake could possibly induce two different perturbations in the ionosphere: one which occurs right above the epicenter and the second one at the conjugate point. It means that the instigator of this second perturbation can follow the magnetic field lines. In Figures 2 and 3, the electron density and the O^+ ion density have again the same variation (not shown).

[7] Figure 4 shows the traces of the orbits corresponding to Figures 1–3. The star on each orbit indicates the position where the density is maximum and one can see that it corresponds to the closest approach to the epicenter for the three events.

4. A Systematic Analysis

[8] Following the observation of the events mentioned above, a systematic study of the ion density in the vicinity of the earthquake's epicenter has been done to check if similar perturbations could be found when there is no seismic activity. The results are displayed in Figure 5. For our study, we use data recorded on orbits with a vertical trace at less than 10° (~1100 km) from the position of the main shock (35.85°S, 72.72°W). As another criterion, nighttime orbits have been used because the daytime orbits of DEMETER are always in the local morning hours and no perturbation is observed. The data have also been selected for the same season from the beginning of January to the end of March during 4 years. When these criteria are satisfied, all available data provided by the IAP instrument on board the DEMETER satellite correspond to about 350 orbits. For each chosen orbit 6 min of data are approximately considered and we have made an array of plasma density where each bin corresponds to the geographic latitude of the satellite with respect to the latitude of the epicenter (noted as 0 on each panel of Figure 5). The white gaps show position in which the given criteria were not satisfied and we do not have any data. These arrays are displayed as function of days before and after 27 February each year, noted as zero on the time axis. Each panel of Figure 5 corresponds to a different year, and Figure 5 (top) is related to 2010 where zero on the time axis corresponds to the earthquake day. Among others, density enhancements shown in Figures 1–3 can be recognized in the 2010 panel. Among the 4 years of data, it can be observed that the plasma density presents maxima only during days preceding the Chile earthquake. Plots similar to Figure 5 have been also done at the same latitude of the earthquake epicenter but at different longitudes (6°–36°E, 96°–126°E, and 186°–216°E) and they do not display any variation. In order to check the magnetic activity and the solar activity, Figure 6 displays the daily sum of the *Kp* indices and the $F_{10.7}$ indices for the same four time intervals as in Figure 5. It can be observed that *Kp* values remain very low (particularly in the 2010 panel) and that $F_{10.7}$ values are also very low due to the fact that we were in an exceptionally long lower part of a solar cycle.

5. Discussions and Conclusions

[9] The presented statistical analysis agrees with previous studies that reported local variations of plasma density in time and position close to coming earthquakes [see, e.g., *Liu et al.*, 2009; *Kon et al.*, 2011]. The seismic effect is of course all the more important as the magnitude is large [*Hobara and Parrot*, 2005]. DEMETER often registers such

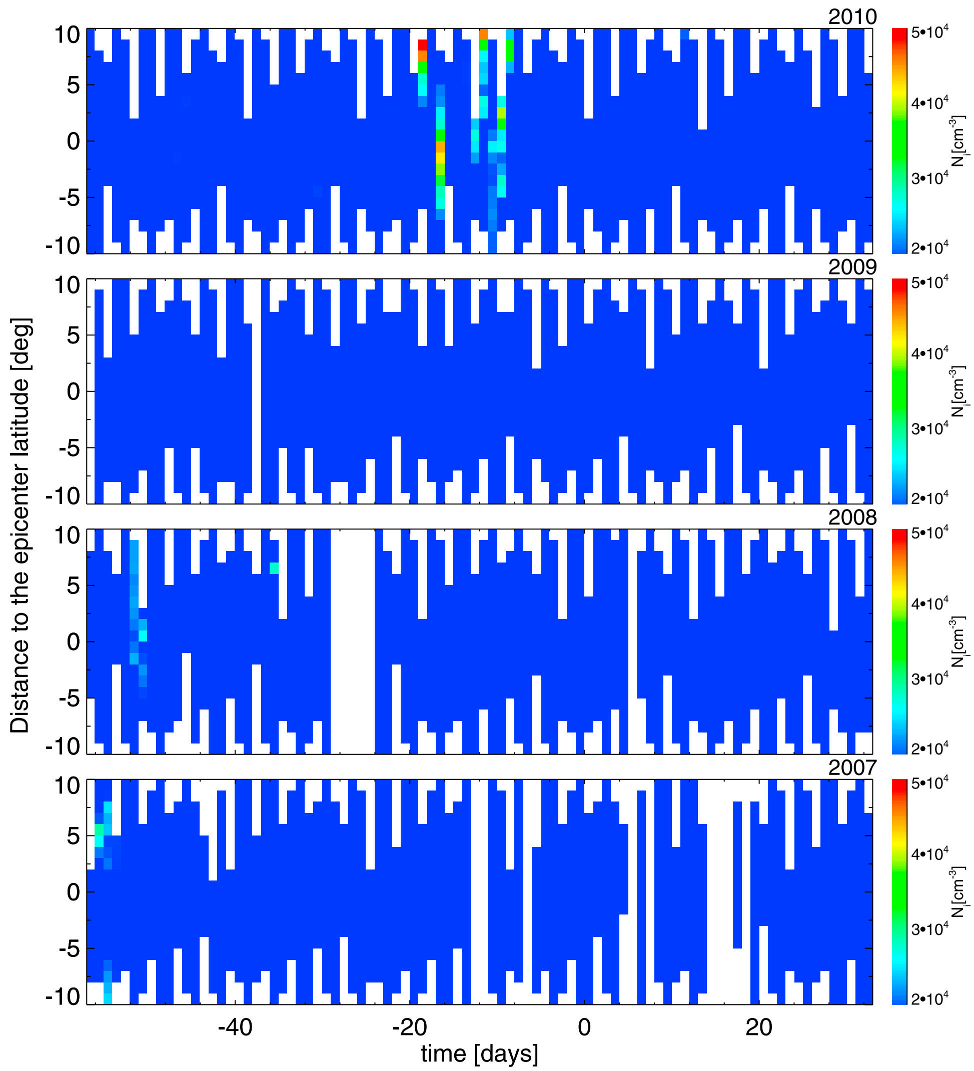

Figure 5. Representation of the data recorded during 4 years in the vicinity of the epicenter of the M_w 8.8 Chile earthquake. Each panel is related to 1 year and represents the plasma density for each day from 1 January to 31 March. The day 0 on the x axis corresponds to 27 February each year (the day of the main shock in 2010). The latitude 0 on the y axis corresponds to the latitude of the epicenter (35.85°S). Only data which are at a distance less than 10° (~1100 km) from the epicenter are shown. The value of the density is color coded according to the color scales on the right. These color scales are identical for all years. The background dark blue color corresponds to values which are mainly around 3000 cm^{-3}.

anomalies before earthquakes. It already demonstrated a statistical link between the apparition of electromagnetic perturbations and the earthquakes with magnitude larger than 5 [*Němec et al.*, 2008]. The various mechanisms mentioned in the introduction will not be discussed in this paper but our observation shown in Figure 3 (a perturbation vertically above the epicenter and another at a point that is geomagnetically linked to the epicenter) indicates that the phenomena could be complex, with a possible involvement of waves and/or charged particles which can be guided by the magnetic field. Even if the mechanism is not known up to now, one must say that electric field generated for example by radon mechanism can penetrate in the lower ionosphere [*Pulinets et al.*, 1998]. If there is a change in the crust at the time of an earthquake, it is certain that it will induce changes at ionospheric levels.

[10] The systematic study over 4 years of measurements has shown that such high increase of plasma density is only observed a few days before the main shock of this powerful Chile earthquake. But, for several reasons, it remains difficult to perform prediction from this potential short-term precursor signal. In general, it is impossible to estimate the time of the earthquakes because these perturbations occur between a few hours and a few weeks before earthquakes. In the past it has been shown [see, e.g., *Tsai et al.*, 2006] that perturbations are observed 1–6 days before large earthquakes. Concerning this Chile event, the observation of density enhancements 10–20 days could be attributed to its

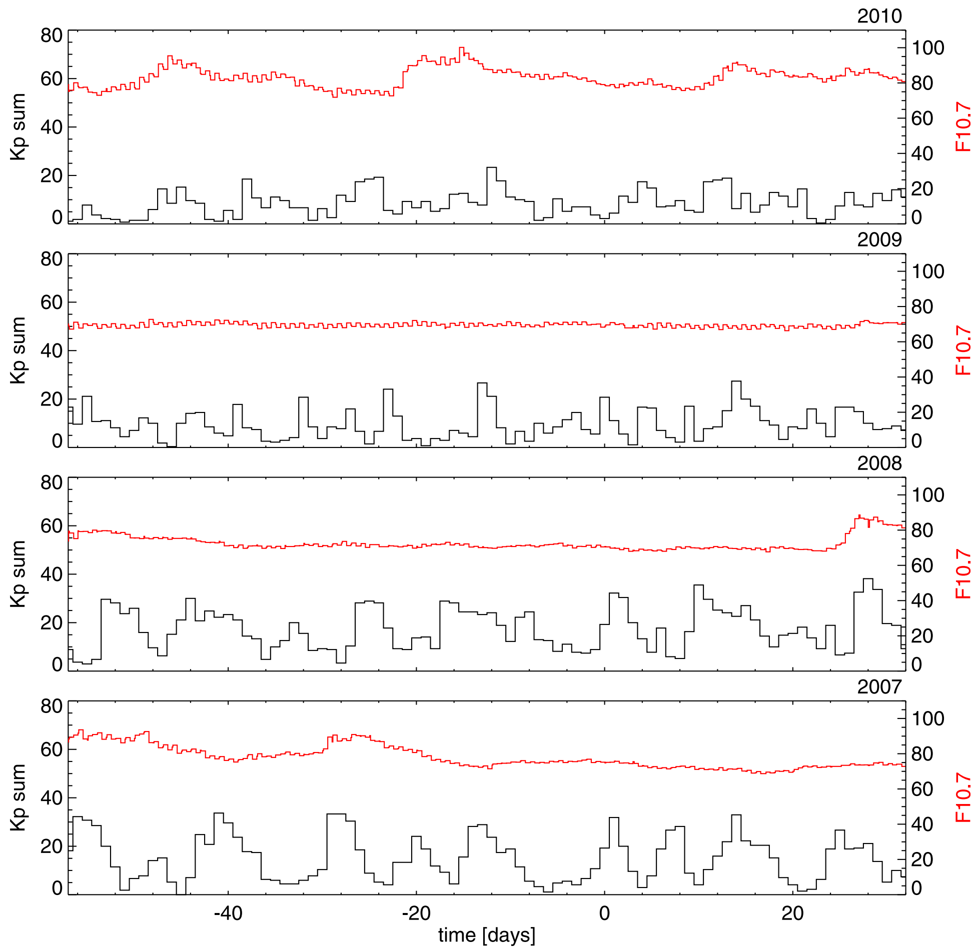

Figure 6. Representation of the sum of the *Kp* (black, left scale) and $F_{10.7}$ (red, right scale) indices recorded during 4 years around the time of the M_w 8.8 Chile earthquake. Each panel is related to 1 year and represents the indices for each day from 1 January to 31 March. The day 0 on the *x* axis corresponds to 27 February each year (the day of the main shock in 2010). *Kp* data are from the Kyoto World Data Center, and $F_{10.7}$ data are from the National Geophysical Data Center (NGDC) of the National Oceanic and Atmospheric Administration (NOAA).

very large and outstanding magnitude. If we consider the current state of our understanding of the observed perturbations as possible precursors of seismic activity, the uncertainties on the predicted position and on the magnitude of the future earthquakes are very large.

[11] There are many scientists over the world working with the DEMETER data. Their objective is to characterize these anomalies and the kind of seismic events they are associated with, to learn how to automatically detect them in the data, to compare their occurrence with the seismic activity in order to understand their origin, and to define criteria which can be used in the future to make predictions. This is a long-term goal of our research, but the signal observed before the M_w 8.8 Chile earthquake will contribute to this task.

[12] **Acknowledgments.** This work was supported by the Centre National d'Etudes Spatiales. It is based on observations with the plasma analyzer IAP embarked on DEMETER. The authors thank J. J. Berthelier, the PI of this instrument, for the use of the data.

[13] Robert Lysak thanks the reviewers for their assistance in evaluating this paper.

References

Asada, T., H. Baba, M. Kawazoe, and M. Sugiura (2001), An attempt to delineate very low frequency electromagnetic signals associated with earthquakes, *Earth Planets Space*, *53*, 55–62.

Berthelier, J. J., M. Godefroy, F. Leblanc, E. Seran, D. Peschard, P. Gilbert, and J. Artru (2006), IAP, the thermal plasma analyzer on DEMETER, *Planet. Space Sci.*, *54*(5), 487–501, doi:10.1016/j.pss.2005.10.018.

Blanc, E. (1985), Observations in the upper atmosphere of infrasonic waves from natural or artificial sources: A summary, *Ann. Geophys.*, *3*, 673–687.

Freund, F. (2009), Stress-activated positive hole charge carriers in rocks and the generation of pre-earthquake signals, in *Electromagnetic Phenomena Associated With Earthquakes*, edited by M. Hayakawa, pp. 41–96, Transworld Res. Network, Trivandrum, India.

Harrison, R. G., K. L. Aplin, and M. J. Rycroft (2010), Atmospheric electricity coupling between earthquake regions and the ionosphere, *J. Atmos. Sol. Terr. Phys.*, *72*, 376–381, doi:10.1016/j.jastp.2009.12.004.

Hattori, K. (2004), ULF geomagnetic changes associated with large earthquakes, *Terr. Atmos. Oceanic Sci.*, *15*, 329–360.

Hobara, Y., and M. Parrot (2005), Ionospheric perturbations linked to a very powerful seismic event, *J. Atmos. Sol. Terr. Phys.*, *67*, 677–685, doi:10.1016/j.jastp.2005.02.006.

Kon, S., M. Nishihashi, and K. Hattori (2011), Ionospheric anomalies possibly associated with $M \geq 6.0$ earthquakes in the Japan area during 1998–2010: Case studies and statistical study, *J. Asian Earth Sci.*, *41*(4–5), 410–420, doi:10.1016/j.jseaes.2010.10.005.

Larkina, V. I., V. V. Migulin, O. A. Molchanov, I. P. Kharkov, A. S. Inchin, and V. B. Schvetcova (1989), Some statistical results on very low frequency radiowave emissions in the upper ionosphere over earthquake zones, *Phys. Earth Planet. Inter.*, *57*, 100–109, doi:10.1016/0031-9201(89)90219-7.

Liu, J. Y., et al. (2006), Giant ionospheric disturbances excited by the *M*9.3 Sumatra earthquake of 26 December 2004, *Geophys. Res. Lett.*, *33*, L02103, doi:10.1029/2005GL023963.

Liu, J. Y., S. W. Chen, Y. C. Chen, H. Y. Yen, C. P. Chang, W. Y. Chang, L. C. Tsai, C. H. Chen, and W. H. Yang (2008), Seismo-ionospheric precursors of the 26 December 2006 *M* 7.0 Pingtung earthquake doublet, *Terr. Atmos. Oceanic Sci.*, *19*, 751–759, doi:10.3319/TAO.2008.19.6.751(PT).

Liu, J. Y., et al. (2009), Seismoionospheric GPS total electron content anomalies observed before the 12 May 2008 *Mw* 7.9 Wenchuan earthquake, *J. Geophys. Res.*, *114*, A04320, doi:10.1029/2008JA013698.

Němec, F., O. Santolík, M. Parrot, and J. J. Berthelier (2008), Spacecraft observations of electromagnetic perturbations connected with seismic activity, *Geophys. Res. Lett.*, *35*, L05109, doi:10.1029/2007GL032517.

Němec, F., O. Santolík, and M. Parrot (2009), Decrease of intensity of ELF/VLF waves observed in the upper ionosphere close to earthquakes: A statistical study, *J. Geophys. Res.*, *114*, A04303, doi:10.1029/2008JA013972.

Norabuena, E. O., T. H. Dixon, S. Stein, and C. G. A. Harrison (1999), Decelerating Nazca-South America and Nazca-Pacific plate motions, *Geophys. Res. Lett.*, *26*(22), 3405–3408, doi:10.1029/1999GL005394.

Parrot, M. (1994), Statistical study of ELF/VLF emissions recorded by a low-altitude satellite during seismic events, *J. Geophys. Res.*, *99*, 23,339–23,347, doi:10.1029/94JA02072.

Parrot, M. (1999), Statistical studies with satellite observations of seismogenic effects, in *Atmospheric and Ionospheric Electromagnetic Phenomena Associated With Earthquakes*, edited by M. Hayakawa, pp. 685–695, Terra Sci., Tokyo.

Parrot, M. (Ed.) (2006), First results of the DEMETER micro-satellite, *Planet. Space Sci.*, *54*(5), pp. 411–557.

Parrot, M., and M. M. Mogilevsky (1989), VLF emissions associated with earthquakes and observed in the ionosphere and the magnetosphere, *Phys. Earth Planet. Inter.*, *57*, 86–99, doi:10.1016/0031-9201(89)90218-5.

Pulinets, S. A., and K. A. Boyarchuk (2004), *Ionospheric Precursors of Earthquakes*, Springer, Hedelberg, New York.

Pulinets, S. A., V. V. Khegai, K. A. Boyarchuk, and A. M. Lomonosov (1998), Atmospheric electric field as a source of ionospheric variability, *Sov. Phys. Usp., Engl. Transl.*, *41*(5), 515–522, doi:10.1070/PU1998v041n05ABEH000399.

Tate, J., and W. Daily (1989), Evidence of electro-seismic phenomena, *Phys. Earth Planet. Inter.*, *57*, 1–10, doi:10.1016/0031-9201(89)90207-0.

Tsai, Y. B., J. Y. Liu, K. F. Ma, Y. H. Yen, K. S. Chen, Y. I. Chen, and C. P. Lee (2006), Precursory phenomena associated with 1999 Chi-Chi earthquake in Taiwan as identified under the iSTEP program, *Phys. Chem. Earth*, *31*, 365–377.

M. Parrot, LPC2E, CNRS, 3A Ave. de la Recherche Scientifique, F-45071 Orléans CEDEX 2, France. (mparrot@cnrs-orleans.fr)

D. Píša and O. Santolík, Faculty of Mathematics and Physics, Charles University, Prague 18000, Czech Republic.